Vertical Bridgman Growth of Sapphire
— Seed crystal shapes and seeding characteristics —

K. Hoshikawa[1], J. Osada[1], Y. Saitou[1], E. Ohba[2], C. Miyagawa[2],
T. Kobayashi[2], J. Yanagisawa[2], M. Shinozuka[2], K. Kanno[3]
Faculty of Engineering, Shinshu University[1],
Fujikoshi Machinery Corp.[2], NEL Crystal Corp.[3]
E-mail: khoshi1@shinshu-u.ac.jp

Abstract

The growth of sapphire by the traditional vertical Bridgman (VB) method was studied by using various shapes of seed crystals and tungsten (W) crucibles shaped to match the seeds. Approximately 2-inch diameter, *c*-axis sapphire single crystals were reproducibly grown from three kinds of seed: thin, tapered and full diameter. Factors relating seed type to single-crystal growth are discussed, including the reproducibility of seeding processes, and the generation and elimination of low-angle grain boundaries (LAGBs). What was learned facilitated the subsequent growth of large-diameter, 3-, 4- and 6-inch, *c*-axis single-crystal sapphires from full-diameter seeds.

Keywords

A2 Bridgman technique, A2 Growth from melt, A2 Seed crystals,
A2 Single crystal growth, B1 Sapphire, B3 Light emitting diodes

1. Introduction

Methods of growing sapphire for the fabrication of GaN-based LED devices have recently been attracting considerable attention. Well known techniques for growing large and high-quality sapphire crystals include the Kyropoulos (KP) [1, 2], heat exchange (HE) [2-4], edge-defined, film-fed growth (EFG) [2, 5-7], and Czochralski (CZ) methods [2, 8]. All these methods have been studied extensively and compared in detail [2, 9-13].

We have investigated sapphire crystal growth using the traditional vertical Bridgman (VB) method, in which the crystals are grown in a crucible with rotation and translation in a hot zone with an appropriate temperature distribution. We first

demonstrated with our VB growth of *c*-axis, 3-inch-diameter sapphire that grown crystals could be easily and nondestructively released from a W crucible and that the crucibles could be reused many times [14]. We also showed that the easy crystal release was due to a gap between the crucible inner wall and the grown crystal formed by differential thermal contraction during cooling to room temperature [14]. Our experimental demonstrations and theoretical confirmations of crucible reusability have received favorable attention for their practical value in the industrial production of large sapphire. The reuse of crucibles has been a very important consideration in the HE and VB methods, in which the alumina melt is solidified in the crucible under crystal shape control.

However, we have not yet presented detailed information about the size and shape of seed crystals, the seeding process with precise temperature control, and the single-crystal growth process after seeding. Reproducible seeding with single-crystal growth was very difficult when we could observe neither the seed crystal nor the growth interface during the seeding process in either the HE or the VB method. In the HE method, a seed crystal placed at the bottom of the crucible is kept from melting by a cooling flow of He [3]. This allows seeding that reproducibly yields single-crystal growth, with the seed crystal remaining unmelted. However, in the VB method, with no special technique to prevent the melting of the seed crystal, it is very important to implement precise temperature measurement and control in the vicinity of the crucible bottom during seeding. It was well known that the difficulty of reproducible seeding for single-crystal growth can be strongly dependent on the shape and size of the seed crystal. For the traditional VB method, however, there are a few reports [14, 15] on the shape and size of seed crystals, and on the details of the seeding process when they are used.

In this paper, we first propose a technique for precise temperature measurement at the crucible bottom in the VB growth furnace and verify its utility in providing reproducible seeding. Then, we examine three representative kinds of seed crystals: thin, tapered and full-diameter seeds, used to grow *c*-axis single-crystal sapphire in the traditional VB growth technique. We discuss their differences with respect to reproducible seeding for single-crystal growth, and the generation and elimination of low-angle grain boundaries (LAGBs) [9] in their seeding processes.

2. Experimental

Fig. 1 shows a diagram of the VB furnace used in our experiment. The

temperature distribution as measured with no crucible present is shown at the right side in the figure. The W crucible is mounted on a crucible shaft that can rotate and also translate vertically. The graphite heater is powered by a radio-frequency coil positioned towards the outer periphery of the carbon-felt heat shield. An argon atmosphere is maintained in the airtight chamber at just over 100 kPa.

Fig. 2 shows the shapes of the seeds and crucibles used in these experiments. The thin seed, the tapered seed and the full-diameter seed are shown in Figs. 2(a), 2(b) and 2(c). The inside of the crucibles in which the sapphire crystals were grown were tapered by a few degrees to make it easy to release the crystal from the crucible [14].

The VB growth processes with these seed crystals and crucibles are as follows. Charging process: the seed and raw materials are placed in the crucible. Melting process: the crucible is elevated into the high-temperature zone and all raw materials are melted. Seeding process: a part of the seed is melted during the slow elevation of the crucible into the high-temperature zone, where the temperature gradient is about 10 ^{o}C/cm. Growth process: the crucible is lowered at 3 mm/h. Cooling process: the crucible is cooled to room temperature as the heating power is reduced to zero.

The VB furnace shown in Fig. 1 was used in the basic examination of seeding and growth of crystals with 2-inch diameter main bodies. However, crystals with diameters greater than 3 inches were grown by using another large-sized resistance-heating furnace described in Reference [14].

The crystals grown were cut and both sides mirror-polished as experimental specimens. Green-laser scattering was used to observe the profile of the seeding interface. A crossed polarizer was used to evaluate the LAGBs. X-ray topography was also used to evaluate the LAGBs, the internal residual stress and the dislocation distribution.

3. Results and Discussion

3.1 Temperature measurement and seeding process

It was very important to achieve satisfactory reproducibility in the seeding process, requiring precise measurement and control of the temperature near the crucible bottom. This was so because the present VB method provides no

mechanism to prevent the melting of the seed crystal, such as the He-gas cooling in the HE method [3, 4].

We constructed a new thermocouple structure to give precise and repeatable measurements in temperatures above 2000°C. Fig. 3 shows a schematic drawing of the thermocouple, which is set between the crucible shaft and the crucible (Fig. 3(a)) and a photograph of the one used in our experiment (Fig. 3(b)). The thermocouple consists of two simple wires, one of 95%W-5%Re and the other 74%W-26%Re, and two W discs to which the wires are firmly connected.

Fig. 4 shows the electric circuit (a) and the equivalent electric circuit (b) of the thermocouple shown in Fig. 3. The thermocouple measured the temperature at the crucible bottom to ±0.5°C at about 2000°C, allowing us to establish the seeding process with high reproducibility in the very low temperature gradient of about 10 °C/cm at temperatures near the melting point of sapphire.

The experimental results confirming the reproducibility of seeding are shown in Table 1. Attaining consistent reproducibility was most difficult for crystals grown using the tapered seed shown in Fig. 2(b). In Table 1, the seeding temperature is the value measured by the thermocouple shown in Fig. 3, and the seeding interface position was defined as the distance from seed bottom to the center of the seeding interface. We could observe the interface by the scattering of a green laser beam from defects accumulated along the seeding interface, as shown in Fig. 5. The seeding temperature corresponded well to the seeding interface position as shown in table 1. Four crystals with seeding temperatures of 2012±1 °C showed seeding interface positions of 20±1 mm, which may indicate acceptable reproducibility in their seeding processes.

3.2 Single-crystal growth from various shapes of seed

Representative crystals grown from each of the three kinds of *c*-axis seeds and crucibles shown in Fig. 2 are shown in Fig. 6. Photographs of as-grown crystal ingots grown from thin, tapered and full-diameter seeds are shown in Fig. 6(a-1), (b-1) and (c-1). The seeding interface profiles detected by green laser scattering from regions indicated by yellow dashed lines in Fig. 6(a-1), (b-1) and (c-1) are shown in Fig. 6(a-2), (b-2) and (c-2). The crossed-polarizer images of the c-plane wafers cut from crystal bodies at the red dashed lines in Fig. 6(a-1), (b-1) and (c-1) are shown in Fig. 6(a-3), (b-3) and (c-3). The features of the growth processes and

characteristics of crystals grown from the three kinds of *c*-axis seeds are described below.

3.2.1 Crystal growth with thin seeds

Reproducible seeding and single-crystal growth processes were established using seed crystals with diameters greater than 20 mm in W crucibles. A typical as-grown crystal ingot is shown in Fig. 7(a). It was found that crystals grown from thin seeds with a diameter of 10 mm could not be released from the crucibles without breaking the crystal body off of the thin-seed portion. A typical as-grown crystal ingot with a sketch of the broken off seed portion is shown in Fig. 7(b). We speculate that crystals grown from small-diameter seeds did not release from the crucibles because of insufficient clearance between the grown crystal and the inner crucible wall at the thin-seed well despite the differential thermal contraction during cooling [14]. We concluded from this experimental study that the diameter of a thin seed must be greater than 20 mm to facilitate release of the seed portion from the seed well of the W crucible, permitting the reuse of the crucible.

Fig. 8 shows X-ray topographic images of a-plane wafers parallel to the growth direction cut from three crystals grown with different seeding positions. LAGBs generated at the periphery of seeding portions are observed in all three crystals. These LAGBs propagated into the crystal bodies. Some LAGBs and residual stress are freshly formed at the shoulder portions in each crystal. We speculate that these LAGBs were caused by large bubbles generated at the interface between the crucible inner wall and the periphery of the grown crystal, or some sticking stress between the crucible inner wall and the crystal surface. On the other hand, the residual stress may be generated by thermal stress at the shoulder portions during cooling. However, most of these LAGBs and residual stresses disappear in the upper portions of the crystal bodies.

Fig. 9 shows X-ray topographic images of a-plane wafers cut from the other two crystals, grown with different shoulder shapes. LAGBs inherited from the seed and residual stress are observed in both crystals. We conclude that both the LAGBs and the residual stress were not significantly affected by the shoulder shape.

Fig. 10 shows X-ray topographic images and a crossed-polarizer image of another crystal grown from a thin seed. The LAGBs inherited from the seed portion are the circular LAGBs in Fig. 10(b). The weak residual stress in Fig. 10(b) may be related to that of the shoulder portion, as shown in Fig. 10(a).

On the other hand, no defects are apparent in the crossed-polarizer image in Fig.

10(c). We considered from the present results that the LAGBs and the residual stress observed in the X-ray topographic images in Fig. 10(a) and (b) are weak LAGBs and residual stresses that are undetectable as defects by crossed-polarizer image.

We conclude that reproducible seeding and single-crystal growth are easily established with thin seeds. While slight LAGBs are generated at the periphery of the seeding interface and inherited in the full-diameter body, and these are not completely eliminated in our growth process.

3.2.2 Crystal growth with tapered seeds

Reproducible seeding processes were established using tapered seeds with an angle of less than 45° and length greater than twice their diameter. Typical results illustrating reproducibility are shown in Table 1 of Section 3.1. We solved the difficult problem of controlling the seeding position to within several millimeters by using a newly developed thermocouple, as shown in Fig. 3.

Fig. 11 shows X-ray topographic images of a-plane wafers and crossed-polarizer images of c-plane wafers cut from three typical crystals grown from *c*-axis tapered seed. We can recognize LAGBs in the X-ray topographic image (a-1) and crossed-polarizer image (a-2). It is considered that the LAGBs were caused by large bubbles generated at the interface between the crucible inner wall and the periphery of the grown crystal. Large bubbles often formed, especially at the tapered crucible inner wall just above the seeding interface. The LAGBs were sometimes caused by these bubbles, being clearly related to their size and shape and the positions at which they formed in the seeding process. Fig. 11(a-1) shows a typical example of what was occasionally encountered. Fig. 11(b-1) shows a typical LAGB generated at the periphery of the seeding portion and propagated into the crystal body. Some LAGBs were also generated at the tapered crucible inner wall, caused by some sticking stress between wall and crystal. Not all of these LAGBs were detectable in crossed-polarizer images, as shown in Fig, 11(b-2). We considered that LAGBs generated at the periphery of the seeding interface were easily eliminated during the broadening growth process along the tapered crucible wall when using *c*-axis tapered seed. Figs. 11(c-1) and (c-2) show an example of an LAGB-free wafer. We are able to grow LAGB-free crystals by optimizing the surface conditions at the crucible inner wall, the seeding interface position and shape, the temperature gradient and the growth rate.

Fig. 12(a) shows a photograph of a 3-inch diameter crystal grown with *c*-axis

tapered seed in a Mo crucible using another large resistance-heating furnace already described in reference [14]. A crossed-polarizer image of a c-plane wafer cut from portion B in Fig. 12(a) is shown in Fig. 12(b). X-ray topographic images of a c-plane wafer cut from portion C and an a-plane wafer cut from portion D in Fig. 12(a) are shown in Fig. 12(c) and Fig. 12(d). Figs. 12(b) and (c) show that LAGB-free wafers could be obtained from a 3-inch diameter crystal grown from *c*-axis tapered seed. Some LAGBs are visible in the seed crystal, and were propagated into the grown crystal as shown in Fig. 12(d). These LAGBs, however, must be progressively eliminated during the growth to the full-diameter crystal body.

We concluded from many investigations of VB growth using tapered seeds that obtaining reproducible seeding was more difficult than with the other two seed types, but that LAGB-free crystal growth was relatively easy to achieve. We attribute this to the combination of the tendency of crystal growth to favor orderliness and the broadening growth process along the tapered crucible wall, together with several specially developed growth techniques.

3.2.3 Crystal growth with full-diameter seed

Reproducible seeding processes were established by using full-diameter seed with a length greater than about half its diameter. Precise temperature measurement and control were also important, to keep the seeding interface position consistent within a very few millimeters.

Fig. 13 shows X-ray topographic images and crossed-polarizer images of two typical crystals, A and B, grown from *c*-axis full-diameter seeds. Figs. 13(a-1) and (b-1) show X-ray topographic images of a-plane wafers cut from regions that include the seeding interface of crystals A and B. Fig. 13(a-2) and (b-2) show X-ray topographic images of c-plane wafers cut from regions grown after seeding of crystals A and B. Fig. 13(a-3) and (b-3) show crossed-polarizer images of c-plane wafers cut from near where wafers (a-2) and (b-2) were cut. The X-ray topographic image in Fig. 13(a-1) shows a typical result of unsuccessful seeding with a full-diameter seed. It is clear in Fig. 13(a-1) that some sub-grain boundaries generated at the seeding interface originated in a twin-boundary in the seed crystal, and new sub-grain boundaries were also generated in the seeding process by imperfect melting of the seed crystal at its central region. It was found from the images in Fig. 13(a-2) and (a-3) that we could not grow single crystals without grain

boundaries with the seeding process shown in Fig. 13(a-1). The X-ray topographic image in Fig. 13(b-1) shows the more usual results, with successful seeding by full-diameter seed. Some LAGBs, however, were generated at the periphery of the seeding interface and were propagated into the periphery of the grown crystal body, as shown in Fig. 13(b-2) and (b-3).

Another X-ray topographic examination with a slightly different diffraction plane (Fig. 13(b-2)) shows that the ring-shaped LAGBs at the periphery of the c-plane had a tilt angle of less than 0.5°.

Fig. 14 is a photograph of 3-, 4- and 6-inch diameter crystals, grown from *c*-axis full-diameter seeds. These crystals were grown with a crucible translation rate of 2 to 3 mm/h, using newly developed and larger VB growth equipment that included a high-temperature furnace with graphite heaters and carbon-felt heat shields [14].

Fig. 15 shows X-ray topographic images of a 3-inch diameter crystal grown from *c*-axis full-diameter seed. X-ray topographic images (a) and (b) show an *a*-plane wafer cut parallel to the growth direction, including the seeding interface portion, and a *c*-plane wafer cut perpendicular to the growth direction in the crystal body grown after seeding. LAGBs generated at the periphery near the seeding interface can be seen in Fig. 15(a) and ring-shaped LAGBs are also visible at the periphery of the c-plane wafer, as shown in Fig. 15(b). We found, however, that the thickness of the ring-shaped LAGB at the periphery of the wafer could decrease to less than several millimeters with improved seeding conditions, such as the shape of the seeding interface, seeding position, and the keeping time of the seeding process.

Fig. 16 shows X-ray topographic and crossed-polarizer images of c-plane wafers cut from a 6-inch diameter crystal grown from a *c*-axis full-diameter seed. Ring-shaped LAGBs are observed in the X-ray topographic image in Fig. 16(a). However, no defects are visible in the crossed-polarizer image in Fig. 16(b).

We concluded from our crystal growth experiments with full-diameter seeds that reproducible seeding and single-crystal growth processes are easily established. On the other hand, we found that the ring-shaped LAGBs at the periphery of the wafer are not eliminated in our growth process, although their width could be reduced to less than several millimeters with improved seeding conditions. Thus the growth of large-diameter, 3-, 4- and 6-inch sapphire single crystals from full-diameter seeds was successful using the traditional VB method.

This section presented results and discussion on seeding processes and how the characteristics of grown crystals relate to the shapes of seed crystals in the VB method, with emphasis on the reuse of W crucibles and the growth of single crystals

without LAGBs. The methods and techniques established in the growth of smaller 2-inch in diameter, *c*-axis crystals can be applied to the growth of larger crystals, as much as 3, 4 and 6 inches in diameter. The development of the present method and techniques to the level of industrial technology is now in progress. The presence of some defects, such as voids, inclusions [16] and dislocations, and their characteristic distribution will be discussed in other papers.

4. Summary

The growth of *c*-axis sapphire by the traditional VB method was examined by using thin, tapered and full-diameter seeds and W crucibles shaped to match the seed crystal. Reproducible seeding processes were established by using precise temperature measurement and control with the help of a newly developed thermocouple.

We found that:

(1) The newly developed thermocouple structure enabled the measurement of the temperature with an accuracy of ±0.5 °C at about 2000 °C near the crucible bottom, in the high-temperature zone of the VB growth furnace.
(2) Highly reproducible seeding was accomplished with the very low temperature gradient of about 10 °C/cm at temperatures near the melting point of sapphire.
(3) The growth of *c*-axis single-crystal sapphires of approximately 2-inch diameter was successful using three types of seeds: thin, tapered and full diameter.

We also found that:

(1) Reproducible seeding for single-crystal growth was relatively easy from thin seeds, compared to the other two types. However, LAGBs generated at the periphery of the seeding interface and inherited by the full-diameter body were not eliminated in the growth process.
(2) Reproducible seeding for single-crystal growth was more difficult from tapered seeds, compared to the other two types. However, LAGB-free crystal growth was possible when growth conditions just after seeding were improved.
(3) In single-crystal growth from full-diameter seed, ring-shaped LAGBs at the periphery of the wafer were not eliminated during the growth process. However,

their width could be decreased to less than several millimeters by improving the seeding conditions.

(4) Finally, large diameter, 3-, 4- and 6-inch sapphire single crystals could be grown from full-diameter seeds by using a newly developed large-sized VB growth furnace.

References

[1] Mikhail Ivanovich Musatov; Journal of Optics Technology 77 (2010) 737.

[2] M.S. Akselrod, F.J. Bruni; Modern trends in crystal growth and new applications of sapphire, Journal of Crystal Growth 360 (2012) 134-145.

[3] F. Schmid, D. Viechnicki; Growth of sapphire disks from the melt by a gradient furnace technique, Journal of American Ceramics Society 53 (1970) 528.

[4] C.P.Khattak, F.Schmid; Growth of the world's largest sapphire crystals, Journal of Crystal Growth 225 (2001) 572-579.

[5] P.I. Antonov, S.P. Nikanorov, V.A. Tatarchenko; The growth of controlled profile crystals by Stepanov's method, Journal of Crystal Growth 42 (1977) 447–452.

[6] H.E.LaBelle Jr.; EFG, the invention and application to sapphire growth, Journal of Crystal Growth 50 (1980) 8-17.

[7] K. Wada, K. Hoshikawa; Growth and characterization of sapphire ribbon crystals, Journal of Crystal Growth 50 (1980) 151–159.

[8] A.E.Paladino, B.D.Roiter; Czochralski growth of sapphire, Journal of the American Ceramic Society 47 (1964) 465.

[9] F.J. Bruni, C.M. Liu and J. Stone-Sundberg; Will Czochralski Growth of Sapphire Once Again Prevail? , ACTA PHYSICA POLONICA A 124-2 (2013) 213-218.

[10] D.C. Harris; A Century of Sapphire Crystal Growth, Proceedings of the 10th DoD Electromagnetic Windows Symposium, Norfolk, Virginia, May 2004.

[11] V.A.Tatartchenko; Sapphire crystal growth and applications, in Bulk Crystal Growth of Electronic, Optical and Optoelectronic Materials, P.Capper (Ed.), John Wiley&Sons Ltd., England, 2005, pp.299-338(Chapter10).

[12] E.R. Dobrovinskaya, L.A. Litvinov, V. Pischik; Sapphire: Material, Manufacturing, Applications; Springer, Berlin, 2009.

[13] E.V.Zharikov; Problems and recent advances in melt crystal growth technology,

Journal of Crystal Growth 360 (2012) 146-154.
[14] C.Miyagawa, T.Kobayashi, T.Taishi, K.Hoshikawa; Demonstration of crack -free *c*-axis sapphire crystal growth using the vertical Bridgman method, Journal of Crystal Growth 372 (2013) 95-99.
[15] K. Hoshikawa, T. Taishi, E. Ohba, C. Miyagawa, T. Kobayashi, J. Yanagisawa, M. Shinozuka; Vertical Bridgman Growth of Sapphire Crystals with Thin-Neck Formation Process, accepted in Journal of Crystal Growth. (http://dx.doi.org/10.1016/j.jcrysgro.2013.12.051)
[16] T. Taishi, T. Kobayashi, M. Shinozuka, E. Ohba, C. Miyagawa, K. Hoshikawa; Morphology and formation mechanism of metallic inclusions in VB-grown sapphire crystals, accepted in J. of Crystal Growth (http://dx.doi.org/10.1016/j.jcrysgro.2013.11.063)

Figure caption

Fig. 1 VB furnace with the temperature distribution as measured without crucible.

Fig. 2 Shapes of seeds and crucibles.

Fig. 3 Schematic drawing of the constructed thermocouple (a) and photograph of the thermocouple used in our experiment (b).

Fig. 4 Electric circuit of constructed thermocouple. (a) electric circuit of the thermocouple shown in Fig. 3 and (b) equivalent electric circuit of Fig. 4(a).

Fig. 5 Seeding interface position measurement. (a) photograph of crystal and (b) seeding interface profile observed by green-laser scanning, with seeding interface position measured as 19mm

Fig. 6 Three representative crystals, grown from thin, tapered and full-diameter seeds. (a-1), (b-1) and (c-1) photographs of as-grown crystal ingots, (a-2), (b-2) and (c-2) seeding interface profiles from the yellow dash enclosed regions in (a-1), (b-1) and (c-1) and (a-3), (b-3) and (c-3) crossed-polarizer images of c-plane wafers from the red dash indicated regions in (a-1), (b-1) and (c-1)

Fig. 7 Crystals grown from seeds with 20mm (a) and 10 mm (b) diameters. Crystal body grown from seed with 10 mm (b) diameter could be released by breaking-off the seed portion.

Fig. 8 X-ray topographic images of 3 crystals grown with different seeding positions.

Fig. 9 X-ray topographic images of two crystals grown with different shoulder shapes.

Fig. 10 X-ray topographic images and crossed-polarizer image of crystal grown with *c*-axis
thin seed. X-ray topographic images (a) and (b) are an a-plane wafer including seed and full-diameter body and a c-plane wafer from the full-diameter region. Photograph (c) is a crossed-polarizer image of the wafer in (b).

Fig. 11 X-ray topographic images and crossed-polarizer images of crystal grown from a *c*-axis tapered seed. X-ray topographic images (a-1), (b-1) and (c-1) are a-plane wafers including seeding interfaces and full-diameter portions. Photographs (a-2), (b-2) and (c-2) are crossed-polarizer images of c-plane wafers from the full diameter portions.

Fig. 12 Photograph of 3-inch diameter crystal grown from *c*-axis tapered seed (a), crossed-polarizer image of c-plane wafer (b) and X-ray topographic images of a c-plane wafer (c) and an a-plane wafer (d) cut from the portions C and D of the crystal shown in (a).

Fig. 13 X-ray topographic images and crossed-polarizer images of two typical crystals A and B, grown from *c*-axis full-diameter seeds.

Fig. 14 Photograph of 3-, 4- and 6-inch diameter crystals grown from *c*-axis full-diameter seeds.

Fig. 15 X-ray topographic images of a 3-inch diameter crystal grown from *c*-axis full-diameter seed (a) and (b) respectively show X-ray topographic images of a-plane and c-plane wafers.

Fig. 16 X-ray topographic image (a) and crossed-polarizer image (b) of a c-plane wafer cut from a 6-inch diameter crystal grown from a *c*-axis full-diameter seed.

Table 1 Reproducibility of seeding process

Fig. 1

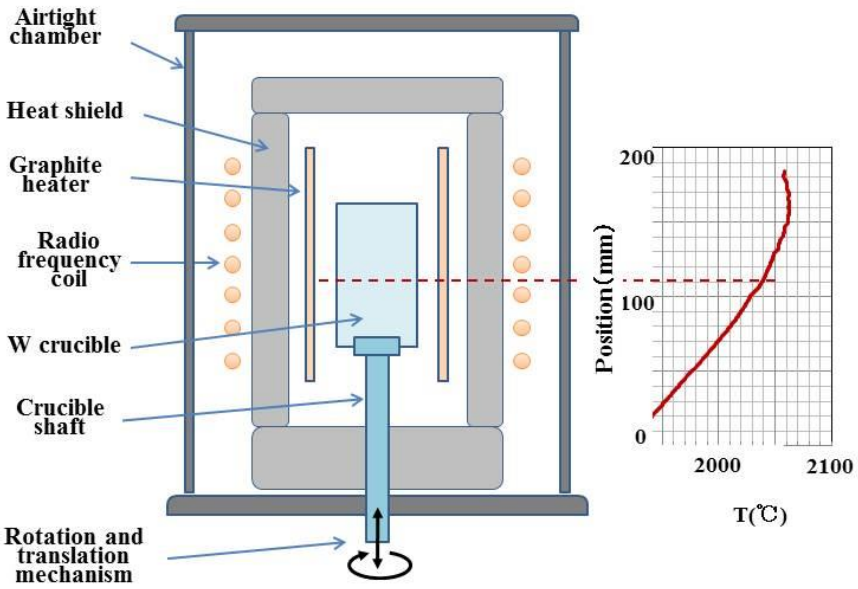

Fig. 2

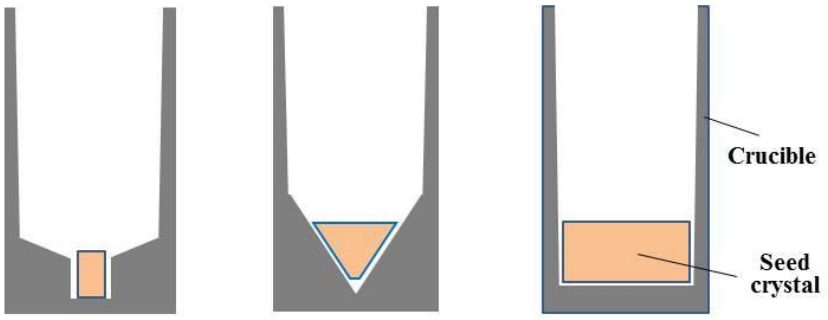

(a) Thin seed (b) Tapered seed (c) Full-diameter seed

Fig. 3

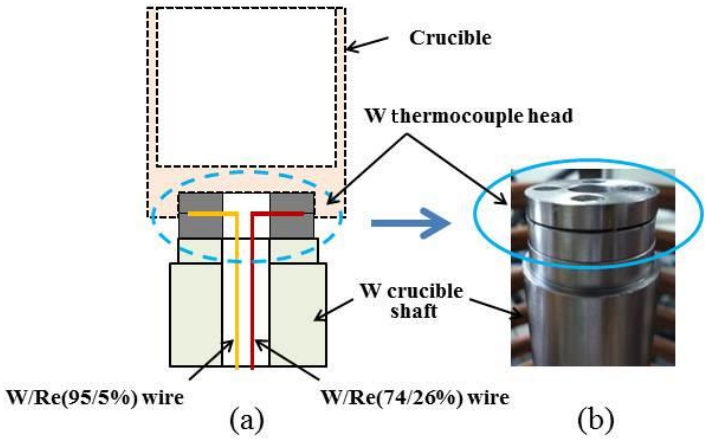
Crucible
W thermocouple head
W crucible shaft
W/Re(95/5%) wire
W/Re(74/26%) wire
(a)
(b)

Fig. 4

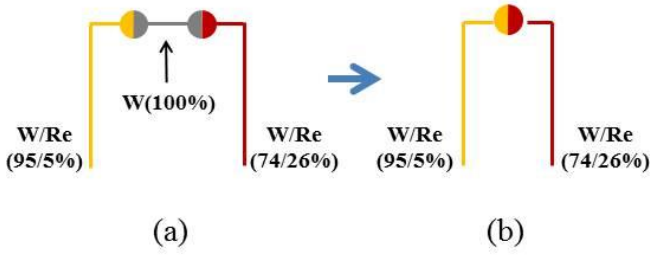
W(100%)
W/Re (95/5%)
W/Re (74/26%)
W/Re (95/5%)
W/Re (74/26%)
(a)
(b)

Fig. 5

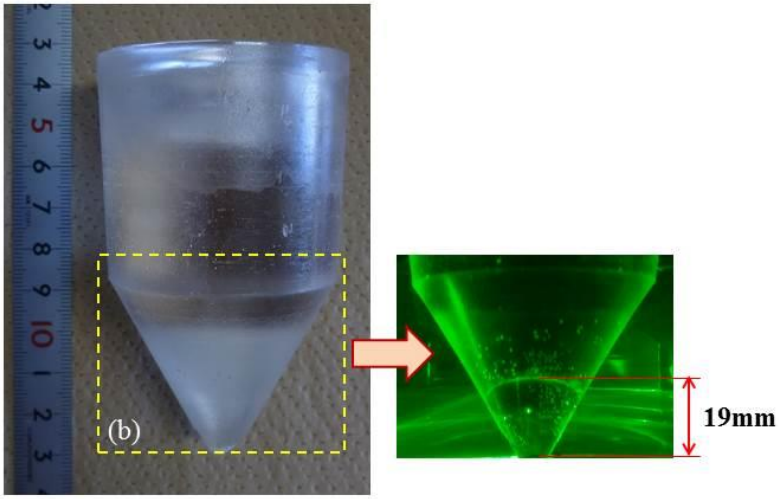

Fig. 6

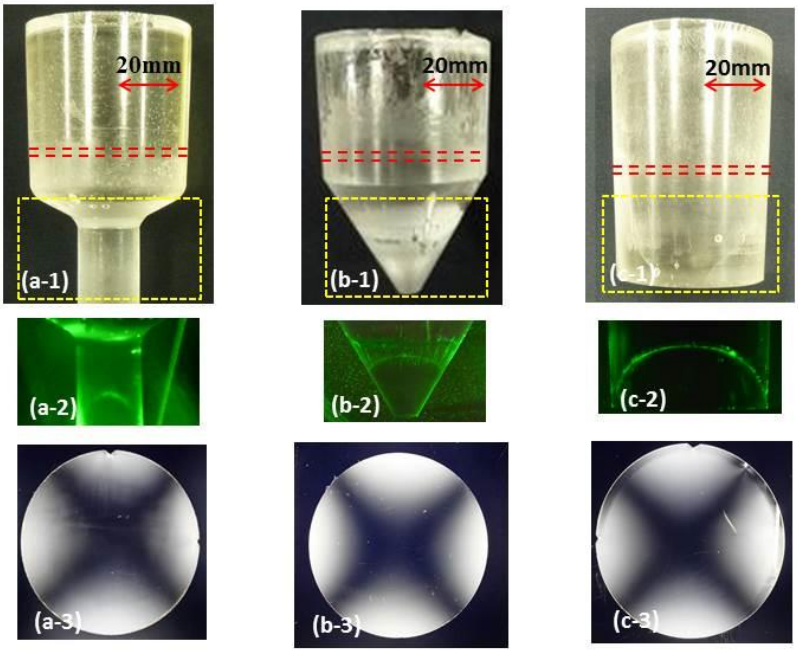

Fig. 7

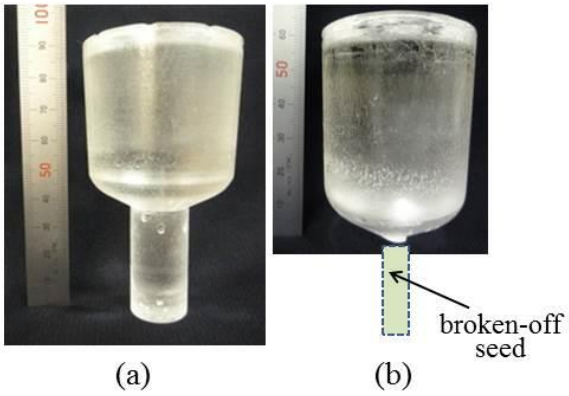
broken-off
seed
(a)
(b)

Fig. 8

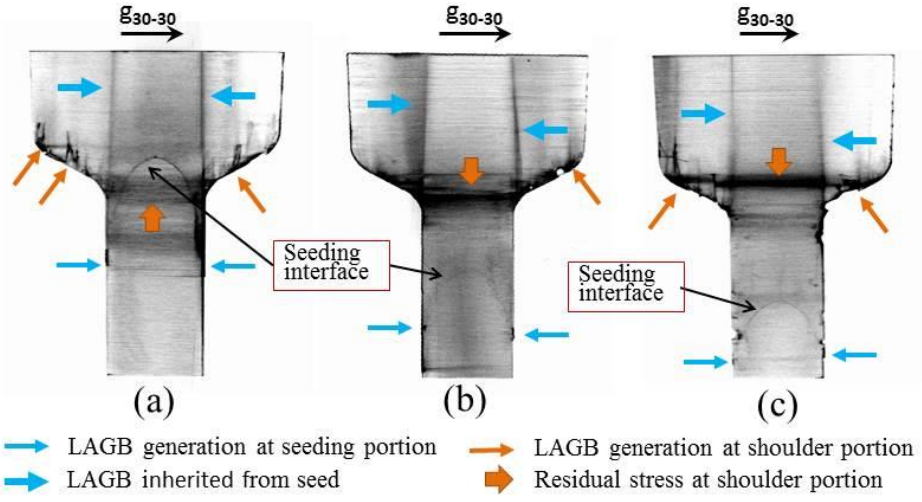
$g_{30\text{-}30}$
$g_{30\text{-}30}$
$g_{30\text{-}30}$
Seeding interface
Seeding interface
(a)
(b)
(c)
LAGB generation at seeding portion
LAGB inherited from seed
LAGB generation at shoulder portion
Residual stress at shoulder portion

Fig. 9

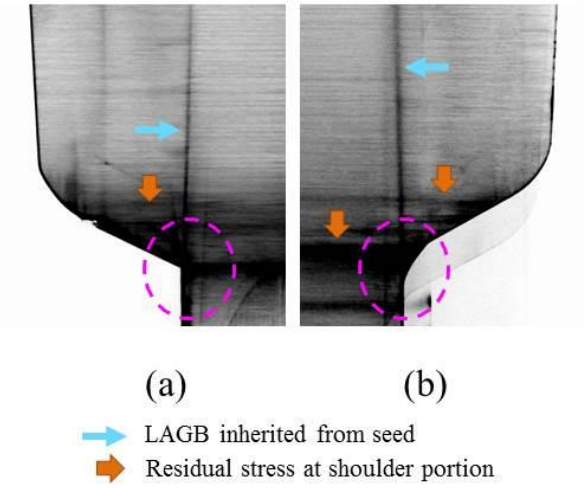
(a)
(b)
LAGB inherited from seed
Residual stress at shoulder portion

Fig. 10

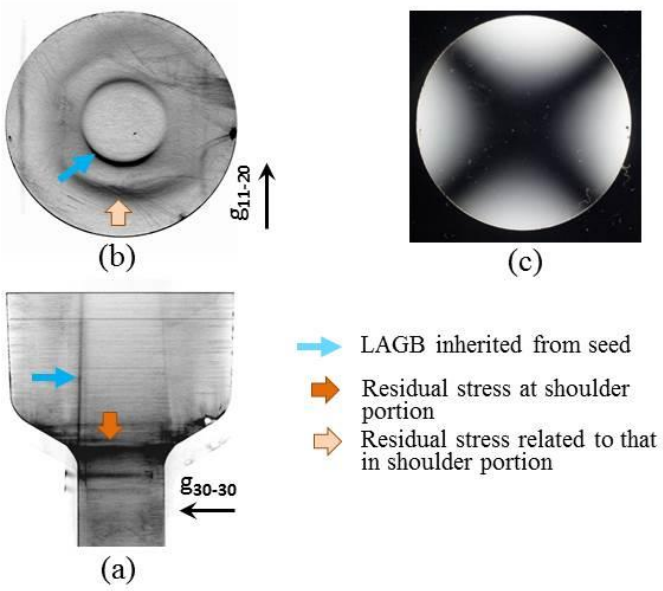
$g_{11\text{-}20}$
(b)
(c)
$g_{30\text{-}30}$
(a)
LAGB inherited from seed
Residual stress at shoulder portion
Residual stress related to that in shoulder portion

Fig. 11

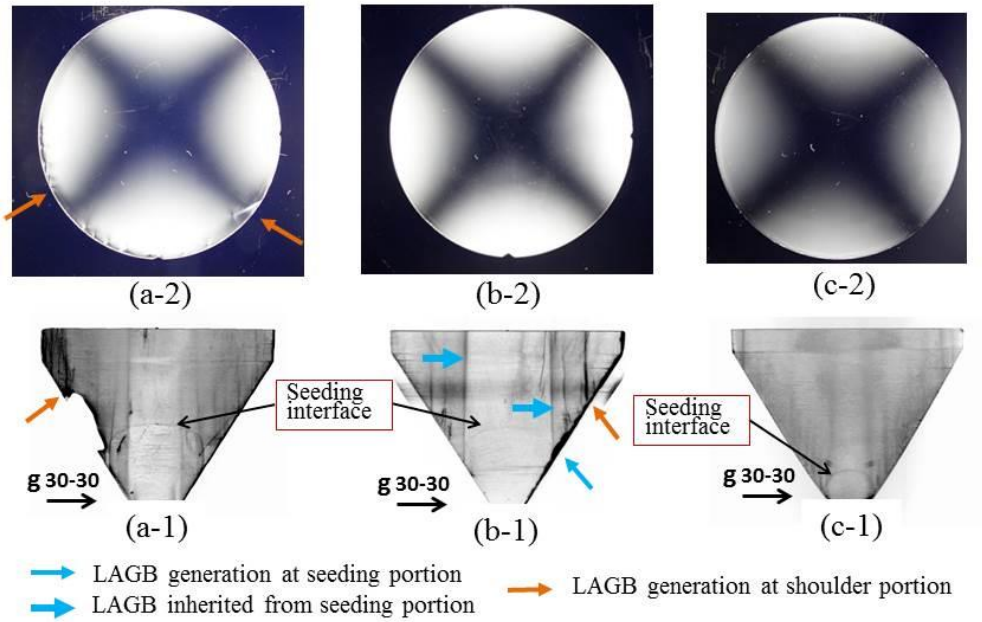
(a-2)
(b-2)
(c-2)
Seeding interface
Seeding interface
g 30-30
g 30-30
g 30-30
(a-1)
(b-1)
(c-1)
LAGB generation at seeding portion
LAGB inherited from seeding portion
LAGB generation at shoulder portion

Fig. 12

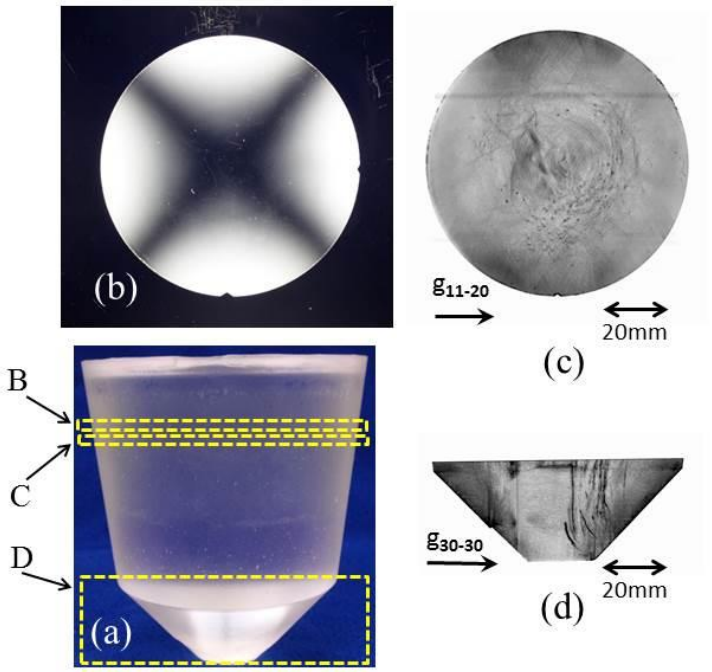
(b)
g11-20
20mm
(c)
B
C
D
(a)
g30-30
20mm
(d)

Fig. 13

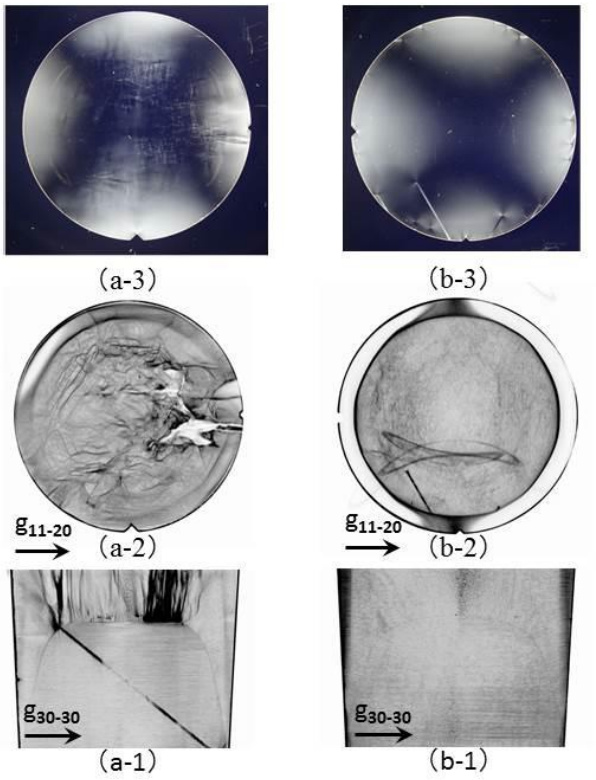

Fig. 14

Fig. 15

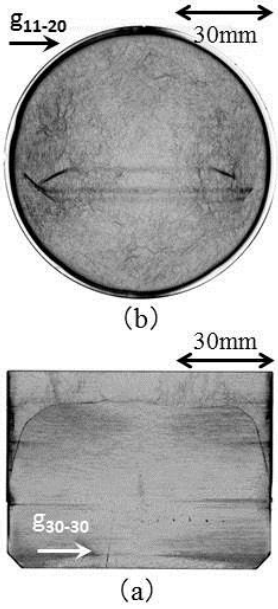

Fig. 16

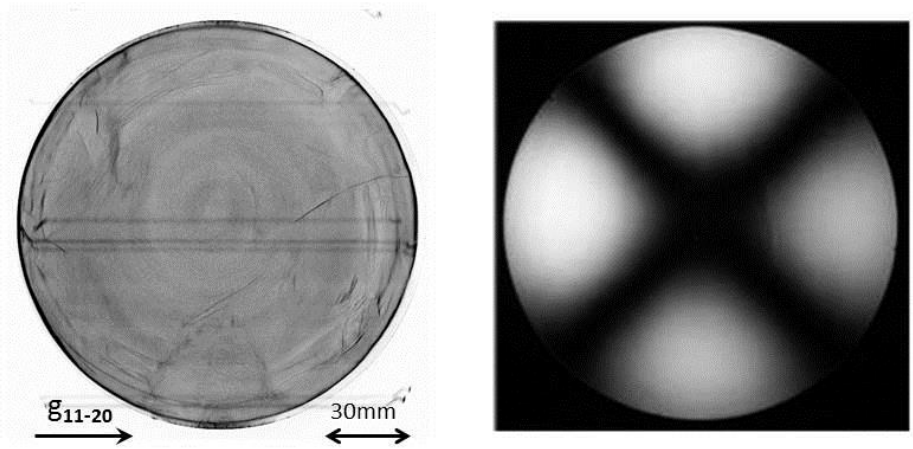

Table 1

Crystal number	No.1	No.2	No.3	No.4
Seeding temperature (℃)	2011.5	2011.0	2012.8	2011.7
Seeding interface position (mm)	21	19	19	20
Photographs of crystal ingots